Title: Flagellin modulates regulation of *Clostridiodes difficile* pathogenesis in the absence of motility

Short title: Flagellin modulates regulation of *Clostridiodes difficile* pathogenesis

Authors: Duolong Zhu[1,2*], Robert Britton[1,2]

Affiliations: [1]Department of Molecular Virology and Microbiology, Baylor College of Medicine, Houston, Texas 77030

[2]Alkek Center for Metagenomics and Microbiome Research, Baylor College of Medicine, Houston, Texas 77030

[*]**Corresponding author:** Duolong Zhu (Email: duolong.zhu@bcm.edu)

Abstract

Clostridioides difficile flagellin (FliC) is associated with toxin gene expression, bacterial colonization and virulence, and is also involved in pleiotropic gene regulation during *in vivo* infection. However, how *fliC* expression is regulated and how FliC modulates *C. difficile* pathogenicity remain unclear. In other bacterial species, FliC participates in a regulatory network with FliW and CsrA to regulate motility. Currently, studies investigating the role of *fliC* in *C. difficile* physiology were performed with motile strains. Despite its canonical role in motility, we found *fliC* is highly conserved in non-motile *C. difficile* strains that have jettisoned most flagellar assembly genes. We therefore investigated the roles of *fliC* in pathogenesis and physiology in the non-motile clade 5 ribotype 078 strain *C. difficile* 1015 (CD1015). We determined that *fliC* was expressed in CD1015 and the regulatory role of *fliC* on toxin production is independent of functional flagella and motility. We showed protein-protein interactions between FliW-FliC and FliW-CsrA using a bacterial two-hybrid system and identified the required binding site for CsrA post-transcriptional regulation in the 5' untranslated region of the *fliC* transcript. Analysis of mutations in *fliC*, *fliW* and *csrA* (and all combinations) on *C. difficile* pathogenesis indicated that FliW plays a central role in *C. difficile* virulence as animals infected with strains carrying a deletion of *fliW* showed decreased survival and increased disease severity. This work highlights that key proteins involved in flagellar biosynthesis retain their regulatory roles in pathogenesis independent of their functions in motility.

Author Summary

C. difficile is a leading cause of nosocomial antibiotic-associated diarrhea in developed countries with many known virulence factors. In several pathogens, motility and virulence are intimately linked by regulatory networks that allow coordination of these processes in pathogenesis and physiology. Regulation of *C. difficle* toxin production by FliC has been demonstrated *in vitro* and *in vivo* and has been proposed to link motility and virulence. Here we show that clinically important, non-motile *C. difficile* strains have conserved FliC and regulatory partners FliW and CsrA, despite lacking the rest of the machinery to produce functional flagella. Our work highlights a novel role for flagellin outside of its role in motility in the pathogenesis and physiology of *C. difficile*.

Introduction

Clostridioides difficile is a Gram-positive, spore-forming, toxin-producing, anaerobic bacterium that is a leading cause of nosocomial antibiotic-associated diarrhea in developed countries [1-3]. Recently, *C. difficile* infection (CDI) reports from the community are rising and becoming a larger portion of total CDI cases [4]. CDI can result in a spectrum of symptoms, ranging from mild diarrhea to pseudomembranous colitis and death [5]. *C. difficile* has many virulence factors, such as toxins, binary toxins, adhesions, and flagella, among which toxin A (TcdA) and toxin B (TcdB) are the major ones [6, 7].

Not only can flagella affect bacterial motility, biofilm formation, and colonization, it has been shown to play a role in virulence, toxin production, and fitness in many bacteria [8-10]. Recently, the flagellin FliC protein (F1-late-stage flagellar gene and the major protein that comprises the flagellum) has been reported to play important roles during *C. difficile* infection in motile strains [9, 11-14]. Aubry et al. [11] reported that disruption of flagellar structural gene *fliC* increased toxin expression. Conversely, disruption of early-stage flagellar genes (F3), such as *fliF*, *fliG*, or *fliM*, led to a significant reduction of toxin production in *C. difficile* 630Δ*erm*. Similarly, Baban et al. [12] reported that *tcdA* expression increased 44.4-fold in a *fliC* gene mutant, while *flgE* (F3 gene) mutation led to 10-fold reduction of *tcdA* expression in *C. difficile* 630Δ*erm*. Interestingly, deletion of other genes involved in flagellar assembly can abolish *C. difficile* motility completely but do not result in a significant change in toxin production that is observed in a *fliC* mutant [11]. Based on previous studies, Stevenson et al. hypothesized that the regulation of the flagellar structural genes on toxin expression could be modulated by the direct change or loss of flagellar genes (such as *fliC* gene deletion) rather than the loss of the functional flagella and bacterial motility [9]. Though the increase of pathogenicity of *fliC* mutant *in vivo* was confirmed and corroborated by several studies, how *fliC* modulates *C. difficile* toxin production and pathogenesis remains unclear.

A partner-switching mechanism Hag-FliW-CsrA which governs flagellin homeostasis and checkpoint of flagellar morphogenesis was first described in *Bacillus subtilis* [15]. Hag (flagellin protein and FliC homolog), FliW (a flagella synthesis regulator), and CsrA (a carbon storage regulator) form a sensitive regulatory feedback loop to regulate flagella biosynthesis in *B. subtilis*. In this feedback regulation, FliW is first released from a FliW-Hag complex following the flagellar assembly checkpoint of hook completion and then binds to CsrA to relieve CsrA-

mediated *hag* translation repression to increase flagellin synthesis concurrent with filament assembly [15]. CsrA is an ancestral protein and has evolved to modulate various physiological processes by regulating mRNA stability and/or translation initiation of target mRNA [16-22]. CsrA typically binds to multiple specific sites that are located near or overlapping the cognate Shine-Dalgarno (SD) sequence in target transcripts [23, 24]. In *B. subtilis*, two CsrA binding sites were identified in the 5'-UTR of *hag* transcripts [24]. Oshiro et al. [25] further quantitated the interactions of FliW, Hag and CsrA, and determined that Hag-FliW-CsrA^{dimer} functions at nearly 1:1:1 stoichiometry in *B. subtilis*.

The regulation of *csrA* on bacterial physiology and carbon metabolism in *C. difficile* 630Δ*erm* was uncovered by overexpressing the *csrA* gene [26]. We previously characterized the pleiotropic roles of FliW and CsrA in *C. difficile* R20291 [27], which supported a similar partner-switching mechanism called FliC-FliW-CsrA. However, more detailed investigations of the FliC-FliW-CsrA molecular mechanism and the modulation of the partner-switching mechanism on pathogenesis in *C. difficile* are needed.

Previous studies have shown that ribotype 078 (Clade 5) *C. difficile* strains lack flagella and bacterial motility [9]. Surprisingly, FliC and FliW are highly conserved in the non-motile clade 5 strains of *C. difficile*, despite their lack of flagella and other genes encoding regulatory and structural genes involved in motility. Here we elucidated how *fliC* modulates *C. difficile* toxin production and pathogenicity in the non-motile strain *C. difficile* 1015 and showed that the FliC-FliW-CsrA regulatory network plays key roles in the pathogenesis and physiology of *C. difficile* independent of flagellar biosynthesis.

Results

fliC, *fliW*, and *csrA* are conserved and expressed in non-motile *C. difficile*

We previously have shown that *fliW* and *csrA* genes are broadly found in *C. difficile* genomes and FliW and CsrA are highly conserved in the different *C. difficile* ribotypes [27]. In *C. difficile* R20291 (RT027 and motile), FliW and CsrA regulate flagellin (FliC) synthesis and bacterial virulence. We found that *fliC*, *fliW*, and *csrA* are conserved in non-motile *C. difficile* strains, despite the fact that many genes involved in flagellar synthesis have been lost [27]. To evaluate the roles of *fliC*, *fliW*, and *csrA* in the non-motile clade 5 (RT078) *C. difficile* strains, we analyzed the conservation of the flagellar regulon genes in *C. difficile* M120 and CD1015 (both

clade 5 RT078 strains). *C. difficile* M120 and CD1015 completely lack early-stage flagellar genes (F3) and only the late-stage flagellar genes (F1, including *fliC*, *fliW*, and *csrA*) and glycosylation genes (F2) were found in the genomes (Fig. 1A and Table S1). We also confirmed that CD1015 was non-motile (unable to swarm and swim) (Fig. 1B). To show *fliC*, *fliW*, and *csrA* are expressed in CD1015, we measured *fliC*, *fliW* and *csrA* transcription and showed they reached maximum expression in early log phase (5 h) with reduced expression as growth entered stationary phase (Fig. 1C). Cotranscription of *fliW* and *csrA* was verified by RT-PCR with CD1015 cDNA (Fig. 1D). These results showed that the *fliC*, *fliW*, and *csrA* genes are expressed in non-motile *C. difficile* and motivated us to explore the roles of these three genes in *C. difficile* pathogenesis, independent of their roles in motility.

Characterization of direct interactions governing the activity of FliC-FliW-CsrA regulation

We previously hypothesized a partner-switching mechanism FliC-FliW-CsrA in *C. difficile* R20291 that was responsible for linking motility and toxin production [27]. Based on the partner-switching mechanism described in *B. subtilis*, we hypothesized that FliC binds FliW, FliW can bind and antagonize the function of CsrA, and CsrA can modulate *fliC* expression post-transcriptionally in CD1015 (Fig. 2A-B). To test the interaction of FliC, FliW, and CsrA, a bacterial two-hybrid system (BACTH system kit) was used [28]. The genes *fliW*, *fliC*, or *csrA* were fused into the N-terminus of plasmid pKNT25 and pUT18, and the C-terminus of plasmid pKT25 and pUT18C, respectively, resulting in plasmids with T25 and T18 tags on N- and C-terminus of FliC, FliW, and CsrA. The reporter strain containing empty plasmids pKNT25 and pUT18 was used as a negative control. As shown in Fig. 2C and Fig. S1, we detected direct interaction between FliW and FliC (FliW-T25+FliC-T18) and interaction between FliW and CsrA (FliW-T25+CsrA-T18), as predicted by our model.

To investigate the post-transcriptional regulation of CsrA on *fliC* expression, we constructed a regulatory reporter plasmid (referred to as P_{lacZ}-UTR-*sfgfp*-P_{tet}-*csrA*) containing two regulatory elements: one is an IPTG-inducible promoter (P_{lacZ}) driving the expression of the 5' untranslated region of *fliC* (UTR) fused upstream of the reporter *sfgfp* gene (P_{lacZ}-UTR-*sfgfp*); the other one is a tetracycline-inducible promoter (P_{tet}) driving the expression of *csrA* (P_{tet}-*csrA*) (Fig. 2D). The strain containing only P_{lacZ}-UTR-*sfgfp* was used as a positive control (P_{lacZ}-UTR-*sfgfp*). As shown in Fig. 2D, induction *csrA* along with *sfgfp* expression (P_{lacZ}-UTR-*sfgfp*-P_{tet}-*csrA*) decreased the fluorescence of the reporter strain dramatically compared to that of the positive

control strain indicating the negative regulation of CsrA on *fliC* expression. To test whether FliW can antagonize CsrA to regulate *fliC* expression, the reporter plasmids containing P_{lacZ}-UTR-*sfgfp* and P_{tet}-*fliW* (or P_{tet}-*fliW-csrA*) were constructed. Our results showed that *fliW-csrA* coexpression (P_{lacZ}-UTR-*sfgfp*-P_{tet}-*fliW-csrA*) can restore fluorescence similar to the positive control strain, indicating FliW antagonizes CsrA (Fig. 2D). Meanwhile, induction of *fliW* along with *sfgfp* expression (P_{lacZ}-UTR-*sfgfp*-P_{tet}-*fliW*) did not affect fluorescence intensity, indicating FliW itself cannot regulate *sfgfp* expression without CsrA (Fig. 2D). These results support a model in which CsrA negatively regulates *fliC* expression by interaction with the UTR of *fliC* and FliW antagonizes CsrA negative regulation. To exclude the impact of CsrA on *fliC* transcription, we measured the *sfgfp* transcription in different reporter strains. As shown in Fig. 2E, no significant difference in *sfgfp* transcription among different reporter strains was detected, which suggests that CsrA regulates *fliC* expression post-transcriptionally.

In *B. subtilis*, 91 bp of the 5' UTR of the *hag* transcript containing two CsrA binding sites has been identified [29]. We analyzed and compared *fliC* and *hag* 5'-UTR structures using the RNAstructure website [30], and found two potential **C**srA **b**inding **s**ites (CBS1: from -45 to -34; CBS2: from -20 to -9, overlapping *fliC* SD sequence) included in the two different predicted hairpin structures (Fig. 2F-H). To test whether the predicted binding sites are required for CsrA post-transcriptional regulation, we deleted either CBS1, CBS2, or both CBS1 and CBS2 (DD: **d**ouble binding sites **d**eletion) in the *fliC* 5'-UTR and assembled the full-length UTR (UTR_F) and the truncated UTRs into the reporter plasmid (P_{lacZ}-UTR_{CBS}-*sfgfp*-P_{tet}-*csrA*) (Fig. 2H). As shown in Fig. 2I, CsrA lost its ability to regulate *fliC* post-transcriptionally when CBS2 (P_{lacZ}-UTR_{CBS1}-P_{tet}-*csrA*) or CBS1-CBS2 (P_{lacZ}-UTR_{DD}-P_{tet}-*csrA*) were deleted but kept similar regulation in the CBS1 deletion reporter strain (P_{lacZ}-UTR_{CBS2}-P_{tet}-*csrA*). These results indicated that CBS2 is required for CsrA post-transcriptional regulation on *fliC* expression. Taken together, we showed that *fliC* is expressed even in the non-motile *C. difficile*, characterized the partner-switching mechanism FliC-FliW-CsrA in *C. difficile*, and identified that the SD sequence (CBS2) is required for CsrA post-transcriptional on *fliC* expression.

FliC-FliW-CsrA negatively regulates toxin production

Multiple reports have shown that *fliC* mutation increases *C. difficile* toxin production and pathogenicity, and that overexpression of *csrA* can also increase toxin production [9, 11, 12]. To test whether the *fliC* gene itself can modulate toxin production and bacterial pathogenicity in

non-motile *C. difficile*, we overexpressed *fliC*, *fliW*, and *csrA* genes in CD1015 and measured the toxin production. As shown in Fig. 3A, all of the overexpressed strains showed significantly decreased toxin production. We were surprised that overexpression of the *csrA* gene decreased *C. difficile* toxin production in CD1015. As this result is contrary to the detected results in CD630 and R20291 [26, 27], it motivated us to explore the detailed roles of *fliC*, *fliW*, and *csrA* in non-motile CD1015.

We constructed deletions of *fliC*, *fliW*, *csrA*, *fliC-fliW*, *fliC-csrA*, *fliW-csrA*, or *fliC-fliW-csrA* in CD1015 using a CRISPR-Cas12a system (Fig. 3B) [31, 32]. Growth profiles of the different mutants were measured in BHIS and TY media and no significant differences in growth nor motility were found Fig. S2A-D. To evaluate the effects of *fliC*, *fliW*, and *csrA* deletion on toxin production, the supernatants of *C. difficile* cultures from TY media at 72 h post-inoculation were collected and toxin levels were measured by ELISA. Only the Δ*fliC*Δ*csrA* strain showed similar toxin production to the wild-type strain while all other mutants significantly increased TcdA and TcdB production (Fig. 3C). As toxin production in most mutants was increased, we measured the transcription of *tcdA* and *tcdB* at 48 h post-inoculation. We found increased *tcdA* and *tcdB* transcripts (Fig. 3D-E), consistent with the results from ELISA analysis.

Collectively, our data indicated that mutations in *fliC* and *fliW* increased toxin production in CD1015, consistent with the previous results reported in motile *C. difficile* [11, 27]. We found that deletion of *csrA* has a positive impact on toxin production in non-motile CD1015 (RT078), while a previous report described a positive impact of *csrA* overexpression in toxin production in motile CD630Δ*erm* (RT012) [26]. Analysis of mutations in *fliC*, *fliW*, and *csrA* (and all combinations) on *C. difficile* toxin production implies that FliW appears to play a central role in the partner-switching mechanism as all mutants carrying a deletion of *fliW* showed increased toxin production.

FliW is a key modulator of *C. difficile* pathogenesis in a non-motile strain

Due to the low sporulation efficiency of CD1015, we prepared vegetative cells to evaluate the effects of the FliC-FliW-CsrA system on CD1015 virulence *in vivo* with a mouse model of CDI. Eighty mice (n=10 per group, 5 female and 5 male mice) were orally challenged with CD1015, Δ*fliC*, Δ*fliW*, Δ*csrA*, Δ*fliC*Δ*fliW*, Δ*fliC*Δ*csrA*, Δ*fliW*Δ*csrA*, or Δ*fliC*Δ*fliW*Δ*csrA* vegetative cells (10^8 CFU/mouse) after antibiotic treatment. As shown in Fig. 4A, mice infected with Δ*fliC*Δ*fliW* (log-rank analysis, P □ 0.001), Δ*fliW* (P □ 0.01), Δ*fliW*Δ*csrA* (P □ 0.01), or Δ*fliC*Δ*fliW*Δ*csrA*

(P 0.05) showed a significant increase in mortality compared to CD1015. Meanwhile, 40% of Δ*fliC* and 30% of Δ*csrA* infected mice succumbed to the severe disease within five days compared to only 10% of CD1015 and Δ*fliC*Δ*csrA* infected mice, which did not reach significance ($P > 0.05$). We scored the severity of disease daily after day 0 using a previously described clinical sickness scoring system (CSS) based on the mice behavioral changes, stool characteristics, and weight loss [33]. The highest CSS score for each mouse within 7 days post-infection was used for CSS comparison between the CD1015 and mutant strains. Our results (Fig. 4B) showed that clinical scores of all derivative mutants except Δ*fliC*Δ*csrA* were higher than that of the parent strain, indicating more serious disease in mice colonized mutants that disrupt FliC-FliW-CsrA regulation.

Our work highlights that key proteins involved in flagellar homeostasis retain their regulatory roles in pathogenesis independent of their functions in motility. Analysis of mutations in *fliC*, *fliW*, and *csrA* (and all combinations) on *C. difficile* pathogenesis indicates that FliW appears to play a central role in the virulence of *C. difficile* as animals infected with strains carrying a deletion of *fliW* all showed decreased survival and increased disease severity.

Disruption of FliC-FliW-CsrA allows *C. difficile* 1015 growth on mannose

Given the central role of CsrA in bacterial carbon metabolism [34-36], we measured the growth profile of Δ*fliC*, Δ*fliW*, and Δ*csrA* mutants on 190 carbon sources using Biolog PM1 and PM2A plates. As shown in Fig. 5A, the three mutants showed significant growth changes in 13 of the 190 carbon substrates, including D-Trehalose, D-Mannose, D-Serine, D-Glucose-6-Phospate, D-Ribose, L-Glutamine, D-Fructose-6-Phosphate, Glycyl-L-Proline, 2-Aminoethanol, Pyruvic acid, Phenylethylamine, D-Sorbitol, and Citramalic acid. Among them, trehalose and mannose led to the maximum growth difference between the parent and mutant strains. We further examined the *C. difficile* growth profile in the different concentrations of trehalose and mannose. CD1015 and mutants were cultured in CDMM media supplemented with 40 mM mannose or 20 mM trehalose, respectively. Our results (Fig. 5B-C and Fig. S3) showed that mannose does not support CD1015 growth in CDMM media but all of the mutants were able to utilize mannose as a carbon source. In trehalose supplemented CDMM media, Δ*fliC*Δ*fliW* and Δ*fliC*Δ*fliW*Δ*csrA* showed similar growth compared to CD1015, while all other mutants displayed delayed cell lysis (Fig. 5D and Fig. S3). In addition, Δ*fliC*, Δ*csrA*, and Δ*fliC*Δ*fliW* reached a higher maximum optical density compared to CD1015 (Fig. 5D).

To learn more about how mutations are affecting trehalose and mannose metabolism, we measured the gene expression of enzymes involved in the breakdown of these sugars. In CD1015, *treA* and *treA2* genes (encoding phosphotrehalase enzymes) participate in trehalose utilization and a mannose-6-phosphate isomerase (*manA*) is predicted to be a key enzyme in mannose metabolism. To analyze the effects of *fliC*, *fliW*, and *csrA* on the expression of these genes, we measured the transcription of *treA*, *treA2*, and *manA* in the deletion mutants and compared them to CD1015. As shown in Fig. 5E, *manA* gene transcription increased significantly in all mutants compared to that of CD1015 at 8 h post-inoculation in 40 mM mannose which could explain a high mannose utilization in the mutants. Meanwhile, Δ*fliW* and Δ*fliC*Δ*fliW* showed increased *treA* transcription and Δ*fliC* and Δ*csrA* showed increased *treA* and *treA2* transcription at 8 h post-inoculation in 20 mM trehalose (Fig. 5F). Together, our data indicates that *fliC*, *fliW*, and *csrA* gene deletions have a significant impact on sugar metabolism.

Δ*fliC*, Δ*fliW*, and Δ*csrA* mutants outcompete CD1015 in the presence of trehalose and mannose

To evaluate the impact of *fliC*, *fliW*, and *csrA* deletions on bacterial fitness in specific carbon sources, *in vitro* competition assays were performed. CD1015 and each mutant were co-cultured in CDMM media supplemented with either 40 mM mannose or 20 mM trehalose and incubated for 12 hours. Primers 1-F/R which can pair to both CD1015 and mutants genomes were used for total competition bacteria detection and primers 42-F/R, 43-F/R, and 2-F/R which can only pair to the wild type genome were used for CD1015 detection (Fig. 6A). As shown in Fig. 6B-D, the abundance of CD1015 accounting for the total bacteria in competition with Δ*fliC*, Δ*fliW*, Δ*csrA* groups significantly decreased at 12 h post-competition growth, which was 22.0, 21.3, and 43.3-fold in 40 mM mannose, and was 10.5, 4.3, and 25.3-fold in 20 mM trehalose compared to the start time (0 h). We also used primers 3-C-F/R to detect *fliC* deletion mutant and 4-C-F/R for *fliW*, *csrA*, and *fliW-csrA* detection (Fig. S4A). Our results (Fig. S4-7) showed that the percentage of CD1015 in total bacteria decreased significantly in competition with Δ*fliC*, Δ*fliW*, and Δ*csrA* mutants which is consistent with the qPCR test results. Our competition data are consistent with the growth profile analysis, indicating Δ*fliC*, Δ*fliW*, and Δ*csrA* mutants outcompete the wild type strain in trehalose and mannose supplemented media, which could lead to better fitness in the host gut environment and cause higher mortality *in vivo*.

Disruption of FliC-FliW-CsrA impairs *C. difficile* sporulation

Motility and carbon utilization are often intertwined with decisions to undergo sporulation, therefore we measured the sporulation efficiency of each mutant with 70:30 sporulation agar plates. As shown in Fig. 7A, the parent strain CD1015 showed a low sporulation efficiency (~5%) after 5 days of incubation on plates. Meanwhile, each single mutant and combinations of mutants showed significantly lower sporulation efficiencies compared to CD1015. Among them, the sporulation efficiency of Δ*csrA* and Δ*fliW*Δ*csrA* were 186 and 384-fold lower than CD1015, respectively. Δ*fliC*Δ*fliW*, Δ*fliC*Δ*csrA*, and Δ*fliC*Δ*fliW*Δ*csrA* sporulation effiencies all decreased more than 10-fold. As *spo0A* plays a key regulatory role in *C. difficile* sporulation process [37], we compared *spo0A* transcription in the mutants and CD1015. Our results (Fig. 7B) showed that the *spo0A* transcription of all derivative mutants were significantly decreased compared to that of CD1015 (P □ 0.0001), which supports the lower sporulation of the mutants.

Discussion

Bacteria have complex regulatory networks that govern the decision to settle in a favorable environment or become motile to find new environments. In pathogens, the decision to make flagella or biofilms is often intimately tied to nutrient acquisition, virulence factor expression, and toxin production [38, 39]. Our previous work and the work of others suggested that the FliC-FliW-CsrA regulatory loop is responsible for coordinating *C. difficile* toxin production and motility in the epidemic ribotype 027 strain R20291 [26, 27]. We were surprised to see that ribotype 078 strains of *C. difficile* have conserved the flagellin (FliC) protein and FliW, despite the fact these strains are non-motile and most of the other flagellar machinery genes have been lost (Fig. 1). This motivated us to explore the role of FliC-FliW-CsrA partner switch on *C. difficile* physiology in the absence of motility and flagellar assembly in the ribotype 078 strain CD1015.

Elegant previous work has elucidated how the Hag-FliW-CsrA regulatory loop modulates flagellin homeostasis and bacterial motility in *B. subtilis* [24, 25]. Here, we first confirmed that *fliC* is expressed in the non-motile CD1015 and showed that *fliC* can have a significant impact on toxin production (Fig. 3). Our data from two-hybrid studies and genetic experiments agree with the proposed model of direct interactions between FliC-FliW and CsrA-FliW with FliC being regulated post-transcriptionally by CsrA (Fig. 2 and Fig. S1). Interestingly, in two predicted CsrA binding sites, only the Shine-Dalgarno sequence (located in CBS2) of *fliC*

transcripts is required for CsrA post-transcriptional regulation, which is distinct from the regulation in *B. subtilis*. However, the export and assembly of flagella in *B. subtilis* is a key player in the complex partner switch mechanism of regulation, which is lost in CD1015 and other *C. difficile* ribotypes that are non-motile and lack flagella.

Currently, the main known function of FliC-FliW-CsrA is to control bacterial motility and the impacts of this regulatory loop on other bacterial phenotypes has been mostly unexplored. In non-motile *C. difficile* strains that lack the machinery to construct flagella, regulation of this network is still intact. By constructing *fliC*, *fliW*, and *csrA* (and all combinations of mutations) mutations in CD1015, we found that the toxin production of Δ*fliC*, Δ*fliW*, Δ*csrA*, Δ*fliC*Δ*fliW*, Δ*fliW*Δ*csrA*, and Δ*fliC*Δ*fliW*Δ*csrA* increased significantly (Fig. 3). There was a good agreement between the levels of toxins produced *in vitro* by the mutants and disease severity *in vivo* (Fig. 4). Notably, mutation of *fliW* alone or in combination with the *fliC* and/or *csrA* resulted in the greatest reduction in survival and increased disease severity score compared to CD1015 and other mutations. We also found the double mutant Δ*fliC*Δ*csrA* was the only mutant that did not increase toxin production *in vitro* and did not result in increased disease severity *in vivo*. These data support that FliW is the key node in regulating toxin production and virulence in the FliC-FliW-CsrA regulatory network. We propose that FliW acts as a negative regulator of toxin production whose activity is regulated by direct interactions with FliC and CsrA. Disruption of the pathway that alters this regulation results in increased interaction between FliW and one of its partners, resulting in less FliW to participate in toxin repression. In *C. difficile* R20291 and *Camplyobacter jejuni*, *fliW* mutations result in lower levels of flagellin, reduced motility, and altered pathogenicity [27, 40, 41]. We currently do not know the mechanistic details of how FliW participates in toxin regulation and more work is needed to elucidate the detailed regulatory roles of FliW in bacterial pathogens (Fig. S8).

C. difficile is an obligate anaerobic pathogen, its pathogenesis relies on the formation of aerotolerant dormant spores and the subsequent germination [42]. In our study, we found that disruption of the FliC-FliW-CsrA regulatory network impaired *C. difficile* sporulation significantly (Fig. 7). Sporulation was dramatically reduced in most of the mutants while toxin production was elevated, like what is observed in other situations in which the decision to produce toxins or initiate sporulation appears to be divergent outcomes [43, 44].

Because CsrA has been shown to regulate multiple aspects of central metabolism in many different bacterial species [17, 45], we also were interested in investigating whether the disruption of this regulatory network had an impact on carbon source metabolism. Recently, an *in vivo* gene expression study of R20291Δ*fliC* strain revealed that *treA*, encoding phosphotrehalase, increased 177-fold in the *fliC* mutant compared to the wild-type strain [13]. Our previous study showed that dietary trehalose can contribute to the virulence of epidemic *C. difficile* [46]. Strikingly, we observed that single mutations in all three genes (*fliC*, *fliW*, *csrA*) were able to confer the ability of CD1015 to grow on the sugar mannose and altered how trehalose is metabolized (Fig. 5-6 and Fig. S3-7). *C. difficile* needs to balance sporulation, toxin production, and nutrient utilization in the infected host to successfully invade and colonize the host gut. In the future, one of the central questions moving forward with this line of research is to identify what additional inputs regulate the FliC-FliW-CsrA to impact *C. difficile* pathogenesis and physiology.

Materials and Methods

Bacteria, plasmids, and culture conditions

Table S2 lists the strains and plasmids used in this study. *C. difficile* strains were cultured in BHIS media (brain heart infusion broth supplemented with 0.5% yeast extract and 0.1% L-cysteine, and 1.5% agar for agar plates) at 37 □ in an anaerobic chamber (90% N_2, 5% H_2, 5% CO_2). For carbon substrate metabolization and Biolog analysis, *C. difficile* strains were cultured in CDMM media supplemented with specific carbon substrates [47, 48]. For spores preparation, *C. difficile* strains were plated on *C. difficile* 70:30 sporulation agar plates (6.3% Bacto peptone, 0.35% proteose peptone, 0.07% $(NH_4)_2SO_4$, 0.106% Tris base, 1.11% BHI, 0.15% g yeast extract, 0.03% L- cysteine, 1.5% agar) and purified as described earlier [49]. To enumerate *C. difficile* CFU in the fecal sample, fecal solutions were plated on adapted TCCFA plates which contain 5 μg/ml lysozyme and 50 μg/ml kanamycin [50]. *Escherichia coli* DH5α, *E. coli* HB101/pRK24, *E. coli* BL21, and *E. coli* BTH101, were grown aerobically at 37 □ in LB media (1% tryptone, 0.5% yeast extract, 1% NaCl). *E. coli* DH5α was used as a cloning host, *E. coli* HB101/pRK24 was used as a conjugation donor host, *E. coli* BL21 was used as a protein expression host, and *E. coli* BTH101 was used as a protein-protein interaction analysis host. Antibiotics were added when needed: for *E. coli*, 20 μg/ml chloramphenicol, 50 μg/ml kanamycin, and 100 μg/ml ampicillin;

for *C. difficile*, 15 μg/ml thiamphenicol, 250 μg/ml D-cycloserine, 50 μg/ml kanamycin, 16 μg/ml cefoxitin, and 500 ng/ml anhydrotetracycline.

DNA manipulations and chemicals

DNA manipulations were carried out according to standard techniques [51]. Plasmids were conjugated into *C. difficile* as described earlier [52]. The DNA markers, PCR product purification kit, DNA gel extraction kit, restriction enzymes, cDNA synthesis kit, and SYBR Green RT-qPCR kit were purchased from Thermo Fisher Scientific (Waltham, USA). PCRs were performed with the high-fidelity DNA polymerase NEB Q5 Master Mix, and PCR products were assembled into target plasmids with NEBuilder HIFI DNA Assembly Master Mix (New England, UK). Primers (Table S3) were purchased from IDT (Coralville, USA). All chemicals were purchased from Sigma (St. Louis, USA) unless those stated otherwise.

FliW, FliC, and CsrA/*csrA* interaction analysis

To analyze the protein-protein interaction of FliC, FliW, and CsrA, a bacterial two-hybrid system (BACTH system kit) was used. We got the BACTH system kit as a gift from Dr. Bouveret (Aix-Marseille University, France) and followed the previously published protocol [28]. Briefly, we digested plasmid pUT18, pUT18C, pKT25, and pKNT25 with *BamH*I. Then *fliW*, *fliC*, and *csrA* genes were amplified and assembled into the N-terminal of plasmid pKNT25 and pUT18, and the C-terminal of plasmid pKT25 and pUT18C with primers 5-10, respectively, resulting in plasmid pKNT25-*fliW* (referred as FliW-T25), pUT18-*fliC* (FliC-T18), pUT18-*csrA*-T18 (CsrA-T18), pKT25-*fliW* (referred as T25-FliW), pUT18C- *fliC* (T18-FliC), and pUT18C- *csrA* (T18-CsrA). Following the two recombinant plasmids encoding the T25-FliW (or FliW-T25) and T18-FliC (or FliC-T18) hybrid proteins were contransformed into competent *E. coli* BTH101 reporter cells for FliW and FliC interaction analysis. Reporter cells containing the T25-FliW (or FliW-T25) and T18-CsrA (or CsrA-T18) hybrid proteins expression plasmids were used for FliW and CsrA interaction analysis. The correct cotransformants were first selected on LB plates with 100 μg/ml ampicillin and 50 μg/ml kanamycin. Then the protein-protein interaction was analyzed by dotting the recombinant BTH101 cultures on LB-X-Gal-IPTG indicator plates. The reporter strain containing empty plasmids pKNT25 and pUT18 was used as a control. The blue colonies indicate a positive result, while the white colonies indicate no interaction between two proteins.

To investigate the post-transcriptional regulation of CsrA on *fliC* expression, we constructed several recombinant reporter plasmids that containing P_{lacZ}-5'UTR-*sfgfp* [5' untranslated region (5'-UTR) of *fliC* transcript and *sfgfp*-6-His (*sfgfp*) fluorescence reporter under the control of P_{lacZ} induction promoter] and P_{tet}-*csrA/fliW/fliW-csrA* (*csrA* or *fliW* or *fliW-csrA* under the control of tetracycline induction promoter P_{tet}) regulation elements with primers 11-19 in pET21b plasmid using NEBuilder HIFI DNA Assembly Master Mix and transformed these reporter plasmids into the expression host *E. coli* BL21. To further identify the CsrA binding sites in 5'UTR of *fliC* transcripts, we analyzed and compared *fliC* and *hag* 5'-UTR structures on RNAstructure website (https://rna.urmc.rochester.edu/RNAstructureWeb/Servers/Predict2/Predict2.html), following we synthesized three truncated 5'UTR of *fliC* and assembled them into pET21b-P_{lacZ}-5'UTR-*sfgfp*-P_{tet}-*csrA* to evaluate the blocking efficiency of CsrA on *sfgfp* expression.

Gene overexpression and deletion in CD1015

Gene *fliC*, *fliW*, and *csrA* were assembled into *EcoR*I-*BamH*I digested plasmid pMTL84153, resulting in overexpression plasmid pMTL84153-*fliC* (referred to as 153-*fliC*), pMTL84153-*fliW* (153-*fliW*), and pMTL84153-*csrA* (153-*csrA*) with primers 20-22, respectively. Gene edit plasmid pDL-1 containing Cas12a (AsCpfI) under control of tetracycline inducing promoter was used for *C. difficile* gene deletion according to the previous reports [31, 32]. The target sgRNA was designed and analyzed on the Cas-OFFinder (http://www.rgenome.net/cas-offinder/) and CINDEL (http://big.hanyang.ac.kr/cindel/) websites. Briefly, constructed gene deletion plasmids (with primers 23-35) from *E. coli* DH5α were transformed into the donor host *E. coli* HB101/pRK24 and were conjugated into *C. difficile* strains subsequently. Transconjugants were selected on BHIS-TKC plates (15 μg/ml thiamphenicol, 50 μg/ml kanamycin, 16 μg/ml cefoxitin) and subcultured into BHIS-Tm broth (15 μg/ml thiamphenicol) to log phase, following the subsequent cultures were diluted with PBS serially and plated on induction plates (BHIS-Tm-ATc: 15 μg/ml thiamphenicol and 500 ng/ml anhydrotetracycline). After 48 h incubation, colony PCR was examined with check primers 1-C-F/R and 2-C-F/R to select the correct gene deletion colonies. Then the deletion plasmid was cured by several passages in BHIS broth without antibiotics. The genome of 1015Δ*fliC* (referred to as Δ*fliC*), 1015Δ*fliW* (Δ*fliW*), 1015Δ*csrA* (Δ*csrA*), 1015Δ*fliC*Δ*fliW* (Δ*fliC*Δ*fliW*), 1015Δ*fliC*Δ*csrA* (Δ*fliC*Δ*csrA*), 1015Δ*fliW*Δ*csrA* (Δ*fliW*Δ*csrA*), and 1015Δ*fliC*Δ*fliW*Δ*csrA* (Δ*fliC*Δ*fliW*Δ*csrA*) were isolated and used as templates

for the PCR test with check primers, and the PCR products were sequenced to confirm the correct gene deletion.

Growth profile and motility assay

C. difficile strains were cultured to an optical density of OD_{600} of 0.8 in BHIS or TY media and were diluted to an OD_{600} of 0.2. Then, 1% of the cultures were inoculated into fresh BHIS or TY, followed by measuring OD_{600} for 48 h.

To analyze the difference in carbon substrate utilization between parent strain and mutants, phenotype microarray plates (PM1 and PM2A) were used to conduct Biolog analysis. Briefly, *C. difficile* strains were cultured to an OD_{600} of 0.6 in BHIS, then 20% of cultures were inoculated into CDMM media with 0.5% glucose and were incubated for another 3 - 4 h [53]. Following, 2 ml of cultures were centrifuged in the chamber and washed three times with CDMM base medium, and finally were resuspended in CDMM media and adjusted into the same OD for Biolog plates and specific carbon source (mannose and trehalose) utilization analysis.

To examine the effect of *fliC* deletion on CD1015 motility, CD1015 and CD1015Δ*fliC* were cultured to an OD_{600} of 0.8. For swarming analysis, 2 µl of cultures were dropped onto 0.2% BHIS agar plates. For swimming analysis, 2 µl of *C. difficile* cultures were penetrated into a soft BHIS agar tube (0.15%). The motility assay plates and tubes were incubated in the anaerobic chamber for 48 h.

Gene transcription and bacteria competition assay

To evaluate toxin production in *C. difficile* strains, 10 ml of *C. difficile* cultures from different strains cultured in TY media were collected at 72 h post incubation. The cultures were adjusted to the same OD_{600} value, centrifuged at 4 □, 8000×*g* for 15 min, filtered with 0.22 µm filters, and then used for ELISA test (EAGLE, CDT35-K01).

For toxin transcription analysis (with primers 37-38), 2 ml of 48 h post inoculated *C. difficile* cultures in TY media were centrifuged at 4 □, 12000×*g* for 5 min for total RNA extraction. To assay *manA*, *treA*, and *treA2* gene expression (with primers 39-40), 5 ml of 8 h post inoculated *C. difficile* cultures in CDMM media supplemented with trehalose or mannose were used for RNA isolation with TRIzol reagent. The transcription of genes were measured by RT-qPCR. All RT-qPCRs were repeated in triplicate, independently. Data were analyzed by using the comparative CT ($2^{-\Delta\Delta CT}$) method with 16s rRNA as a control (with primers 36).

To compare the fitness of CD1015 and mutants in specific carbon substrates, *in vitro* competition assays were conducted. The same CFU of CD1015, Δ*fliC*, Δ*fliW*, and Δ*csrA* from the log phase were collected, centrifuged, and washed three times with CDMM base media in the anaerobic chamber. Following, 10^7 CFU of CD1015 was mixed with the same CFU of Δ*fliC*, Δ*fliW*, and Δ*csrA*, respectively. The mixed seed cultures were then inoculated into CDMM media supplemented with mannose or trehalose. After 12 h of post-inoculation, 100 µl of mixed cultures were serially dilueted and plated on BHIS plates for colony PCR test with primers 3-C-F/R and 4-C-F/R. Meanwhile, the total genome from mixed cultures were isolated and detected by qPCR with primer pairs 1, 2, 42, and 43 for competition analysis. In the colony PCR test, the percentage of CD1015 in the total bacteria was calculated as: CFU_{1015}/CFU_{total}. In the qPCR test, the fold change of CD1015 accounting for total bacteria was calculated as: $2^{(\Delta CT_{12h}-\Delta CT_{0h})}$, $\Delta CT = CT_{1015}-CT_{total}$. Among them, CT_{1015} was acquired by primers 42-F/R in Δ*fliC*, or 43-F/R in Δ*fliW*, or 2-F/R in Δ*csrA* that only paired to the deleted gene sequence, and CT_{total} was acquired by primers 1-F/R paired to the remaining part of *fliC* gene after deletion. ΔCT_0 was calculated with genome from the mixed seed cultures at 0 h.

Bacterial virulence of mutants in the mouse model of CDI

C57BL/6 female and male mice (6 weeks old) were ordered from The Jackson Laboratory, Ellsworth, ME. All studies were approved by the Institutional Animal Care and Use Committee of Baylor College of Medicine. The experimental design and antibiotic administration were conducted as described earlier [54]. Briefly, 80 mice were divided into 8 groups in 16 cages and each mouse was challenged with 10^8 of *C. difficile* vegetative cells after orally administered antibiotic cocktail (kanamycin 0.4 mg/ml, gentamicin 0.035 mg/ml, colistin 0.042 mg/ml, metronidazole 0.215 mg/ml, and vancomycin 0.045 mg/ml) in drinking water for 6 days. After 6 days of antibiotic treatment, all mice were given autoclaved water for 2 days, followed by one dose of clindamycin (10 mg/kg, intraperitoneal route) 24 h before *C. difficile* challenge (Day 0). The mice were monitored daily for a week for changes in weight, diarrhea, stool characteristics, behavior, and mortality. All survived mice were humanely euthanized on day 7 of post *C. difficile* challenge.

Mice fecal pellets at post challenge days 1, 3, and 5 were collected from each mouse and were transformed into the anaerobic chamber as fast as possible. Following, the feces were

diluted with PBS at a final concentration of 30 mg/ml and 100 μl of diluted feces were plated on TCCFA (5 μg/ml lysozyme and 50 μg/ml kanamycin added additionally) plates to enumerate the total CFU of *C. difficile*. To calculate the spores CFU in the feces, the diluted feces solution were heated at 65□ for 30 min, then plated on TCCFA plates as well. To evaluate toxin tilter in feces, 30 mg/ml of the fecal solution was used for TcdA and TcdB ELISA analysis.

Sporulation assay

C. difficile sporulation and germination analysis were conducted as reported earlier [55]. For *C. difficile* sporulation analysis, *C. difficile* strains were cultured on *C. difficile* 70:30 sporulation agar plates for 5 days, following bacterial lawns were scraped from plates and resuspended in PBS. Afterward, CFU of cultures resuspended in PBS was counted on BHIS plates with 0.1% TA for sporulation ratio analysis. The sporulation ratio was calculated as CFU (65 □ heated, 30 min) / CFU (not heated). To analyze the transcription of *spo0A* in the sporulation process, total RNA from *C. difficile* strains at 48 h post incubation on 70:30 sporulation agar plates were extracted and used for RT-qPCR test with primers 44.

Statistical analysis

The reported experiments were conducted in independent biological triplicates, and each sample was additionally taken in technical triplicates. Animal survivals were analyzed by Kaplan-Meier survival analysis and compared by the Log-Rank test. One-way analysis of variance (ANOVA) with post-hoc Tukey test was used for more than two groups comparison. Results were expressed as mean ± standard error of the mean. Differences were considered statistically significant if $P < 0.05$ (*).

Acknowledgments

This work was supported by the National Institutes of Health (NIH) grants to R.A.B. (U01AI124290 and R01AI123278). We thank Dr. Bouveret at Aix-Marseille University, France for gifting us the BACTH system kit. We also thank Dr. Katherine Jayne Wozniak for her mindful revision and comments.

References

1. Lawson PA, Citron DM, Tyrrell KL, Finegold SM. Reclassification of Clostridium difficile as Clostridioides difficile (Hall and O'Toole 1935) Prevot 1938. Anaerobe. 2016;40:95-9. Epub 2016/07/03. doi: 10.1016/j.anaerobe.2016.06.008. PubMed PMID: 27370902.
2. Oren A, Garrity GM. Notification of changes in taxonomic opinion previously published outside the IJSEM. Int J Syst Evol Micr. 2018;68(7):2137-8. PubMed PMID: WOS:000437232500002.
3. Sebaihia M, Wren BW, Mullany P, Fairweather NF, Minton N, Stabler R, et al. The multidrug-resistant human pathogen Clostridium difficile has a highly mobile, mosaic genome. Nat Genet. 2006;38(7):779-86. Epub 2006/06/29. doi: 10.1038/ng1830. PubMed PMID: 16804543.
4. Fu Y, Luo Y, Grinspan AM. Epidemiology of community-acquired and recurrent Clostridioides difficile infection. Therap Adv Gastroenterol. 2021;14:17562848211016248. Epub 2021/06/08. doi: 10.1177/17562848211016248. PubMed PMID: 34093740; PubMed Central PMCID: PMCPMC8141977.
5. Lessa FC, Gould CV, McDonald LC. Current Status of Clostridium difficile Infection Epidemiology. Clin Infect Dis. 2012;55:S65-S70. PubMed PMID: WOS:000306879000001.
6. Lyras D, O'Connor JR, Howarth PM, Sambol SP, Carter GP, Phumoonna T, et al. Toxin B is essential for virulence of Clostridium difficile. Nature. 2009;458(7242):1176-9. Epub 2009/03/03. doi: 10.1038/nature07822. PubMed PMID: 19252482; PubMed Central PMCID: PMCPMC2679968.
7. Kuehne SA, Cartman ST, Heap JT, Kelly ML, Cockayne A, Minton NP. The role of toxin A and toxin B in Clostridium difficile infection. Nature. 2010;467(7316):711-3. Epub 2010/09/17. doi: 10.1038/nature09397. PubMed PMID: 20844489.
8. Harshey RM. Bacterial motility on a surface: many ways to a common goal. Annu Rev Microbiol. 2003;57:249-73. Epub 2003/10/07. doi: 10.1146/annurev.micro.57.030502.091014. PubMed PMID: 14527279.
9. Stevenson E, Minton NP, Kuehne SA. The role of flagella in Clostridium difficile pathogenicity. Trends Microbiol. 2015;23(5):275-82. Epub 2015/02/11. doi: 10.1016/j.tim.2015.01.004. PubMed PMID: 25659185.

10. Duan Q, Zhou M, Zhu L, Zhu G. Flagella and bacterial pathogenicity. J Basic Microbiol. 2013;53(1):1-8. Epub 2012/02/24. doi: 10.1002/jobm.201100335. PubMed PMID: 22359233.

11. Aubry A, Hussack G, Chen W, KuoLee R, Twine SM, Fulton KM, et al. Modulation of toxin production by the flagellar regulon in Clostridium difficile. Infect Immun. 2012;80(10):3521-32. Epub 2012/08/02. doi: 10.1128/IAI.00224-12. PubMed PMID: 22851750; PubMed Central PMCID: PMCPMC3457548.

12. Baban ST, Kuehne SA, Barketi-Klai A, Cartman ST, Kelly ML, Hardie KR, et al. The role of flagella in Clostridium difficile pathogenesis: comparison between a non-epidemic and an epidemic strain. PLoS One. 2013;8(9):e73026. Epub 2013/10/03. doi: 10.1371/journal.pone.0073026. PubMed PMID: 24086268; PubMed Central PMCID: PMCPMC3781105.

13. Barketi-Klai A, Monot M, Hoys S, Lambert-Bordes S, Kuehne SA, Minton N, et al. The flagellin FliC of Clostridium difficile is responsible for pleiotropic gene regulation during in vivo infection. PLoS One. 2014;9(5):e96876. Epub 2014/05/21. doi: 10.1371/journal.pone.0096876. PubMed PMID: 24841151; PubMed Central PMCID: PMCPMC4026244.

14. Tasteyre A, Barc MC, Collignon A, Boureau H, Karjalainen T. Role of FliC and FliD flagellar proteins of Clostridium difficile in adherence and gut colonization. Infect Immun. 2001;69(12):7937-40. Epub 2001/11/14. doi: 10.1128/IAI.69.12.7937-7940.2001. PubMed PMID: 11705981; PubMed Central PMCID: PMCPMC98895.

15. Mukherjee S, Yakhnin H, Kysela D, Sokoloski J, Babitzke P, Kearns DB. CsrA-FliW interaction governs flagellin homeostasis and a checkpoint on flagellar morphogenesis in Bacillus subtilis. Mol Microbiol. 2011;82(2):447-61. Epub 2011/09/08. doi: 10.1111/j.1365-2958.2011.07822.x. PubMed PMID: 21895793; PubMed Central PMCID: PMCPMC3192257.

16. Romeo T, Gong M, Liu MY, Brun-Zinkernagel AM. Identification and molecular characterization of csrA, a pleiotropic gene from Escherichia coli that affects glycogen biosynthesis, gluconeogenesis, cell size, and surface properties. J Bacteriol. 1993;175(15):4744-55. Epub 1993/08/01. doi: 10.1128/jb.175.15.4744-4755.1993. PubMed PMID: 8393005; PubMed Central PMCID: PMCPMC204926.

17. Timmermans J, Van Melderen L. Post-transcriptional global regulation by CsrA in bacteria. Cell Mol Life Sci. 2010;67(17):2897-908. Epub 2010/05/07. doi: 10.1007/s00018-010-0381-z. PubMed PMID: 20446015.

18. Liu MY, Yang H, Romeo T. The product of the pleiotropic Escherichia coli gene csrA modulates glycogen biosynthesis via effects on mRNA stability. J Bacteriol. 1995;177(10):2663-72. Epub 1995/05/01. doi: 10.1128/jb.177.10.2663-2672.1995. PubMed PMID: 7751274; PubMed Central PMCID: PMCPMC176935.

19. Sabnis NA, Yang H, Romeo T. Pleiotropic regulation of central carbohydrate metabolism in Escherichia coli via the gene csrA. J Biol Chem. 1995;270(49):29096-104. Epub 1995/12/08. doi: 10.1074/jbc.270.49.29096. PubMed PMID: 7493933.

20. Lawhon SD, Frye JG, Suyemoto M, Porwollik S, McClelland M, Altier C. Global regulation by CsrA in Salmonella typhimurium. Mol Microbiol. 2003;48(6):1633-45. Epub 2003/06/07. doi: 10.1046/j.1365-2958.2003.03535.x. PubMed PMID: 12791144.

21. Lucchetti-Miganeh C, Burrowes E, Baysse C, Ermel G. The post-transcriptional regulator CsrA plays a central role in the adaptation of bacterial pathogens to different stages of infection in animal hosts. Microbiology. 2008;154(Pt 1):16-29. Epub 2008/01/05. doi: 10.1099/mic.0.2007/012286-0. PubMed PMID: 18174122.

22. Ferreiro MD, Nogales J, Farias GA, Olmedilla A, Sanjuan J, Gallegos MT. Multiple CsrA Proteins Control Key Virulence Traits in Pseudomonas syringae pv. tomato DC3000. Mol Plant Microbe Interact. 2018;31(5):525-36. Epub 2017/12/21. doi: 10.1094/MPMI-09-17-0232-R. PubMed PMID: 29261011.
23. Sorger-Domenigg T, Sonnleitner E, Kaberdin VR, Blasi U. Distinct and overlapping binding sites of Pseudomonas aeruginosa Hfq and RsmA proteins on the non-coding RNA RsmY. Biochem Biophys Res Commun. 2007;352(3):769-73. Epub 2006/12/05. doi: 10.1016/j.bbrc.2006.11.084. PubMed PMID: 17141182.
24. Yakhnin H, Pandit P, Petty TJ, Baker CS, Romeo T, Babitzke P. CsrA of Bacillus subtilis regulates translation initiation of the gene encoding the flagellin protein (hag) by blocking ribosome binding. Mol Microbiol. 2007;64(6):1605-20. Epub 2007/06/09. doi: 10.1111/j.1365-2958.2007.05765.x. PubMed PMID: 17555441.
25. Oshiro RT, Rajendren S, Hundley HA, Kearns DB. Robust Stoichiometry of FliW-CsrA Governs Flagellin Homeostasis and Cytoplasmic Organization in Bacillus subtilis. mBio. 2019;10(3). Epub 2019/05/23. doi: 10.1128/mBio.00533-19. PubMed PMID: 31113895; PubMed Central PMCID: PMCPMC6529632.
26. Gu H, Qi H, Chen S, Shi K, Wang H, Wang J. Carbon storage regulator CsrA plays important roles in multiple virulence-associated processes of Clostridium difficile. Microb Pathog. 2018;121:303-9. Epub 2018/06/03. doi: 10.1016/j.micpath.2018.05.052. PubMed PMID: 29859293.
27. Zhu D, Wang S, Sun X. FliW and CsrA Govern Flagellin (FliC) Synthesis and Play Pleiotropic Roles in Virulence and Physiology of Clostridioides difficile R20291. Front Microbiol. 2021;12:735616. Epub 2021/10/23. doi: 10.3389/fmicb.2021.735616. PubMed PMID: 34675903; PubMed Central PMCID: PMCPMC8523840.
28. Battesti A, Bouveret E. The bacterial two-hybrid system based on adenylate cyclase reconstitution in Escherichia coli. Methods. 2012;58(4):325-34. Epub 2012/07/31. doi: 10.1016/j.ymeth.2012.07.018. PubMed PMID: 22841567.
29. Dubey AK, Baker CS, Romeo T, Babitzke P. RNA sequence and secondary structure participate in high-affinity CsrA-RNA interaction. RNA. 2005;11(10):1579-87. Epub 2005/09/01. doi: 10.1261/rna.2990205. PubMed PMID: 16131593; PubMed Central PMCID: PMCPMC1370842.
30. Tan Z, Fu Y, Sharma G, Mathews DH. TurboFold II: RNA structural alignment and secondary structure prediction informed by multiple homologs. Nucleic Acids Res. 2017;45(20):11570-81. Epub 2017/10/17. doi: 10.1093/nar/gkx815. PubMed PMID: 29036420; PubMed Central PMCID: PMCPMC5714223.
31. Zhu D, Patabendige H, Tomlinson BR, Wang S, Hussain S, Flores D, et al. Cwl0971, a novel peptidoglycan hydrolase, plays pleiotropic roles in Clostridioides difficile R20291. Environ Microbiol. 2021;23(9):5222-38. Epub 2021/04/25. doi: 10.1111/1462-2920.15529. PubMed PMID: 33893759.
32. Hong W, Zhang J, Cui G, Wang L, Wang Y. Multiplexed CRISPR-Cpf1-Mediated Genome Editing in Clostridium difficile toward the Understanding of Pathogenesis of C. difficile Infection. ACS Synth Biol. 2018;7(6):1588-600. Epub 2018/06/05. doi: 10.1021/acssynbio.8b00087. PubMed PMID: 29863336.
33. Shelby RD, Tengberg N, Conces M, Olson JK, Navarro JB, Bailey MT, et al. Development of a Standardized Scoring System to Assess a Murine Model of Clostridium

difficile Colitis. J Invest Surg. 2020;33(10):887-95. Epub 2019/03/21. doi: 10.1080/08941939.2019.1571129. PubMed PMID: 30892111.
34. Baker CS, Morozov I, Suzuki K, Romeo T, Babitzke P. CsrA regulates glycogen biosynthesis by preventing translation of glgC in Escherichia coli. Mol Microbiol. 2002;44(6):1599-610. Epub 2002/06/18. doi: 10.1046/j.1365-2958.2002.02982.x. PubMed PMID: 12067347.
35. Hauslein I, Sahr T, Escoll P, Klausner N, Eisenreich W, Buchrieser C. Legionella pneumophila CsrA regulates a metabolic switch from amino acid to glycerolipid metabolism. Open Biol. 2017;7(11). Epub 2017/11/03. doi: 10.1098/rsob.170149. PubMed PMID: 29093212; PubMed Central PMCID: PMCPMC5717341.
36. Sahr T, Rusniok C, Impens F, Oliva G, Sismeiro O, Coppee JY, et al. The Legionella pneumophila genome evolved to accommodate multiple regulatory mechanisms controlled by the CsrA-system. PLoS Genet. 2017;13(2):e1006629. Epub 2017/02/18. doi: 10.1371/journal.pgen.1006629. PubMed PMID: 28212376; PubMed Central PMCID: PMCPMC5338858.
37. Underwood S, Guan S, Vijayasubhash V, Baines SD, Graham L, Lewis RJ, et al. Characterization of the sporulation initiation pathway of Clostridium difficile and its role in toxin production. J Bacteriol. 2009;191(23):7296-305. Epub 2009/09/29. doi: 10.1128/JB.00882-09. PubMed PMID: 19783633; PubMed Central PMCID: PMCPMC2786572.
38. Purcell EB, McKee RW, Courson DS, Garrett EM, McBride SM, Cheney RE, et al. A Nutrient-Regulated Cyclic Diguanylate Phosphodiesterase Controls Clostridium difficile Biofilm and Toxin Production during Stationary Phase. Infect Immun. 2017;85(9). Epub 2017/06/28. doi: 10.1128/IAI.00347-17. PubMed PMID: 28652311; PubMed Central PMCID: PMCPMC5563577.
39. Allocati N, Masulli M, Di Ilio C, De Laurenzi V. Die for the community: an overview of programmed cell death in bacteria. Cell Death Dis. 2015;6:e1609. Epub 2015/01/23. doi: 10.1038/cddis.2014.570. PubMed PMID: 25611384; PubMed Central PMCID: PMCPMC4669768.
40. Radomska KA, Ordonez SR, Wosten MM, Wagenaar JA, van Putten JP. Feedback control of Campylobacter jejuni flagellin levels through reciprocal binding of FliW to flagellin and the global regulator CsrA. Mol Microbiol. 2016;102(2):207-20. Epub 2016/06/30. doi: 10.1111/mmi.13455. PubMed PMID: 27353476.
41. Li J, Gulbronson CJ, Bogacz M, Hendrixson DR, Thompson SA. FliW controls growth-phase expression of Campylobacter jejuni flagellar and non-flagellar proteins via the post-transcriptional regulator CsrA. Microbiology (Reading). 2018;164(10):1308-19. Epub 2018/08/17. doi: 10.1099/mic.0.000704. PubMed PMID: 30113298; PubMed Central PMCID: PMCPMC6600343.
42. Britton RA, Young VB. Interaction between the intestinal microbiota and host in Clostridium difficile colonization resistance. Trends Microbiol. 2012;20(7):313-9. Epub 2012/05/19. doi: 10.1016/j.tim.2012.04.001. PubMed PMID: 22595318; PubMed Central PMCID: PMCPMC3408078.
43. Edwards AN, Krall EG, McBride SM. Strain-Dependent RstA Regulation of Clostridioides difficile Toxin Production and Sporulation. J Bacteriol. 2020;202(2). Epub 2019/10/30. doi: 10.1128/JB.00586-19. PubMed PMID: 31659010; PubMed Central PMCID: PMCPMC6941533.
44. Clark AE, Adamson CC, Carothers KE, Roxas BAP, Viswanathan VK, Vedantam G. The Alternative Sigma Factor SigL Influences Clostridioides difficile Toxin Production, Sporulation,

and Cell Surface Properties. Front Microbiol. 2022;13:871152. Epub 2022/06/01. doi: 10.3389/fmicb.2022.871152. PubMed PMID: 35633701; PubMed Central PMCID: PMCPMC9130780.

45. Romeo T, Babitzke P. Global Regulation by CsrA and Its RNA Antagonists. Microbiol Spectr. 2018;6(2). Epub 2018/03/25. doi: 10.1128/microbiolspec.RWR-0009-2017. PubMed PMID: 29573256; PubMed Central PMCID: PMCPMC5868435.

46. Collins J, Robinson C, Danhof H, Knetsch CW, van Leeuwen HC, Lawley TD, et al. Dietary trehalose enhances virulence of epidemic Clostridium difficile. Nature. 2018;553(7688):291-4. Epub 2018/01/09. doi: 10.1038/nature25178. PubMed PMID: 29310122; PubMed Central PMCID: PMCPMC5984069.

47. Karasawa T, Ikoma S, Yamakawa K, Nakamura S. A defined growth medium for Clostridium difficile. Microbiology (Reading). 1995;141 (Pt 2):371-5. Epub 1995/02/01. doi: 10.1099/13500872-141-2-371. PubMed PMID: 7704267.

48. Midani FS, Collins J, Britton RA. AMiGA: Software for Automated Analysis of Microbial Growth Assays. mSystems. 2021;6(4):e0050821. Epub 2021/07/14. doi: 10.1128/mSystems.00508-21. PubMed PMID: 34254821; PubMed Central PMCID: PMCPMC8409736.

49. Perez J, Springthorpe VS, Sattar SA. Clospore: A Liquid Medium for Producing High Titers of Semi-Purified Spores of Clostridium difficile. J Aoac Int. 2011;94(2):618-26. PubMed PMID: WOS:000289544500031.

50. Wilson KH, Kennedy MJ, Fekety FR. Use of sodium taurocholate to enhance spore recovery on a medium selective for Clostridium difficile. J Clin Microbiol. 1982;15(3):443-6. Epub 1982/03/01. doi: 10.1128/jcm.15.3.443-446.1982. PubMed PMID: 7076817; PubMed Central PMCID: PMCPMC272115.

51. Chong L. Molecular cloning - A laboratory manual, 3rd edition. Science. 2001;292(5516):446-. PubMed PMID: WOS:000168187300027.

52. Heap JT, Kuehne SA, Ehsaan M, Cartman ST, Cooksley CM, Scott JC, et al. The ClosTron: Mutagenesis in Clostridium refined and streamlined. J Microbiol Meth. 2010;80(1):49-55. PubMed PMID: WOS:000273846600006.

53. Theriot CM, Koenigsknecht MJ, Carlson PE, Jr., Hatton GE, Nelson AM, Li B, et al. Antibiotic-induced shifts in the mouse gut microbiome and metabolome increase susceptibility to Clostridium difficile infection. Nature communications. 2014;5:3114. doi: 10.1038/ncomms4114. PubMed PMID: 24445449; PubMed Central PMCID: PMC3950275.

54. Sun X, Wang H, Zhang Y, Chen K, Davis B, Feng H. Mouse relapse model of Clostridium difficile infection. Infect Immun. 2011;79(7):2856-64. Epub 2011/05/18. doi: 10.1128/IAI.01336-10. PubMed PMID: 21576341; PubMed Central PMCID: PMCPMC3191975.

55. Zhu D, Bullock J, He Y, Sun X. Cwp22, a novel peptidoglycan cross-linking enzyme, plays pleiotropic roles in Clostridioides difficile. Environ Microbiol. 2019;21(8):3076-90. Epub 2019/06/08. doi: 10.1111/1462-2920.14706. PubMed PMID: 31173438.

Figures

Main figure legends

Fig. 1 Non-motile clade 5 (ribotype 078) *C. difficile* conserves and expresses *fliC*, *fliW*, and *csrA*.

(A) Schematic representation of conserved late-stage flagellar (F1) and glycosylation (F2) genes in the non-motile *C. difficile*. (B) Comparison of CD1015 and R20291 motility. (C) Transcription of *fliC* and *csrA* in CD1015 growth. (D) Co-transcription verification of *fliW* and *csrA* genes by RT-PCR. M: DNA ladder; 1-3: CD1015 genomic DNA was used as PCR template; 4-6: CD1015 cDNA was used as PCR template. 1 and 4: *fliW* PCR test; 2 and 5: *csrA* PCR test; 3 and 6: *fliW-csrA* PCR test. Bars stand for mean ± SEM (**$P < 0.01$, ***$P < 0.001$). Differences were considered statistically significant if $P < 0.05$ (*). One-way ANOVA with post-hoc Tukey test was used for statistical significance.

Fig. 2 Characterization of direct interactions of FliC-FliW-CsrA in *C. difficile*.

(A-B) Schematic representation of modulation of FliC, FliW, and CsrA/csrA in *C. difficile*. In the FliC-FliW-CsrA regulatory loop, FliC binds FliW, FliW binds CsrA, and CsrA regulates *fliC* post-transcriptionally through binding 5' untranslated region of *fliC* transcripts. (C) Protein-

protein interaction test of FliC-FliW and FliW-CsrA *in vitro* using a bacterial two-hybrid system. Reporter BTH101 containing pKNT25 and pUT18 was used as a control. BTH101 containing pKNT25-*fliW* (FliW-T25) and pUT18-*fliC* (FliC-T18) was used for FliC and FliW interaction test. BTH101 containing pKNT25-*fliW* (FliW-T25) and pUT18-*csrA* (CsrA-T18) was used for FliC and FliW interaction test. 1, 2, 4, and 8 μl of reporter strain were dotted on LB+IPTG+X-gal indication plates. (D-E) Regulation of CsrA on 5'UTR of *fliC* transcripts. Reporter plasmid pET21b-P_{lacZ}-UTR-*sfgfp*-P_{tet}-*csrA* (or *fliW* or *fliW-csrA*) was constructed, following the fluorescence of reporter strains with different recombinant plasmids were determined (D). Transcription of *sfgfp* in the different recombinant reporter strains (E). (F-G) Structure comparison of *B. subtilis* 5'-UTR of *hag* (F) and CD1015 5'-UTR of *fliC* (G). RNAstructure dynalign results were calculated (calculate the lowest free energy secondary structures common to two unaligned sequences). (H-I) Identification of required binding sites for CsrA post-transcriptional regulation in 5'UTR of *fliC* transcripts. Three truncated 5'UTRs of *fliC* were assembled into the reporter plasmid, respectively (H), and subsequently the fluorescence of reporter strains with different truncated 5'UTR plasmids were analyzed (I). Bars stand for mean ± SEM. Differences were considered statistically significant if $P < 0.05$ (*). One-way ANOVA with post-hoc Tukey test was used for statistical significance.

Fig. 3 FliC-FliW-CsrA negatively regulates toxin expression.

(A) Comparison of toxin production in CD1015-pMTL84153 (CD1015-E) and *fliC* (CD1015-153-*fliC*), *fliW* (CD1015-153-*fliW*), and *csrA* (CD1015-153-*csrA*) overexpression strains. (B) Deletion of UTR-*fliC*, *fliW*, *csrA*, and *fliW-csrA*. 1-C-F/R were used to verify *fliC* deletion and 2-C-F/R were used to test *fliW*, *csrA*, and *fliW-csrA* deletion. M: DNA ladder; 1 and 3: CD1015 genome as PCR template; 2: CD1015Δ*fliC* (Δ*fliC*) genome test; 4: CD1015Δ*fliW* (Δ*fliW*) genome test; 5: CD1015Δ*csrA* (Δ*csrA*) genome test; 6: CD1015Δ*fliW*Δ*csrA* (Δ*fliW*Δ*csrA*) genome test. (C) Toxin concentration in the supernatants of CD1015 and its derivative mutants detected by ELISA. (D) Transcription of *tcdA* and *tcdB* in CD1015 and its derivative mutants detected by RT-qPCR. (E) Fold change of toxin production and transcription compared to those of CD1015 based on C and D data. Bars stand for mean ± SEM. * means the significant difference of experimental strain compared to CD1015-E or CD1015 (*$P < 0.05$, **$P < 0.01$, ***$P < 0.001$, ****$P < 0.0001$). One-way ANOVA with post-hoc Tukey test was used for statistical significance.

Fig. 4 FliC-FliW-CsrA modulates RT078 *C. difficile* 1015 virulence in a mouse model of CDI.

(A) Survival curve of CD1015 and different mutants in a CDI mouse model. Animal survivals were analyzed by Kaplan-Meier survival analysis and compared by the Log-Rank test. Differences were considered statistically significant if $P < 0.05$ (*$P < 0.05$, **$P < 0.01$, ***$P < 0.001$). (B) Disease severity in mice. Clinical sickness scoring system was used to evaluate the mice disease severity. The highest CSS score for each mouse within 7 days post infection was used for CSS comparison in different *C. difficile* strains. * means the significant difference of experimental strain compared to CD1015 (*$P < 0.05$, **$P < 0.01$, ***$P < 0.001$). One-way ANOVA with post-hoc Tukey test was used for statistical significance.

Fig. 5 Disruption of FliC-FliW-CsrA allows *C. difficile* 1015 growth on mannose.

(A) Carrying capacity [*K*, the maximum growth supported by the environment, *K*-log = ln(OD_max)-ln(OD_initial)] of growth profile of CD1015, Δ*fliC*, Δ*fliW*, and Δ*csrA* in Biolog PM1 and PM2A plates. (B-F) Growth curves of CD1015 and its derivative mutants in CDMM media without any added carbon source (B), 40 mM mannose (C), and 20 mM trehalose (D). (E) *manA* transcription of CD1015 and its derivative mutants at 8 h post-inoculation in 40 mM mannose. (F) *treA* and *treA2* transcription of CD1015 and its derivative mutants at 8 h post-inoculation in 20 mM trehalose. Bars stand for mean ± SEM. * means the significant difference of experimental strain compared to CD1015 (*$P < 0.05$, **$P < 0.01$, ***$P < 0.001$, ****$P < 0.0001$). One-way ANOVA with post-hoc Tukey test was used for statistical significance.

Fig. 6 Δ*fliC*, Δ*fliW*, and Δ*csrA* mutants outcompete CD1015 in the presence of trehalose and mannose.

(A) Primers used for the qPCR in the competition test. (B-D) Competition of CD1015 with Δ*fliC*, Δ*fliW*, and Δ*csrA*. Bars stand for mean ± SEM. * means the significant difference of CD1015 abundance in the competition mixtures compared to that of at 0 h (*$P < 0.05$, **$P < 0.01$, ***$P < 0.001$). One-way ANOVA with post-hoc Tukey test was used for statistical significance.

Fig. 7. Disruption of FliC-FliW-CsrA impairs *C. difficile* sporulation.

(A) Sporulation assay. *C. difficile* strains were cultured on 70:30 sporulation agar plates for 5 days, following the scraped cultures were 10-fold diluted and plated on BHIS plates with 0.1%

TA to detect sporulation ratio. The sporulation ratio was calculated as CFU (65 □ heated, 30 min) / CFU (not heated). (B) Transcription of *spo0A*. Total RNA from *C. difficile* strains at 48 h post incubation was extracted for the RT-qPCR test. Bars stand for mean ± SEM. * means the significant difference of experimental strain compared to CD1015 (*$P < 0.05$, **$P < 0.01$, ****$P < 0.0001$). One-way ANOVA with post-hoc Tukey test was used for statistical significance.

Supplementary figure legends

Fig. S1 Protein-protein interaction of FliC, FliW, and CsrA *in vitro*.

(A-H) *fliW*, *fliC*, and *csrA* genes were fused into the N-terminal of plasmid pKNT25 and pUT18, and the C-terminal of plasmid pKT25 and pUT18C, respectively, resulting in plasmid pKNT25-*fliW* (referred as FliW-T25), pUT18-*fliC* (FliC-T18), pUT18-*csrA* (CsrA-T18), pKT25-*fliW* (referred as T25-FliW), pUT18C-*fliC* (T18-FliC), and pUT18C-*csrA* (T18-CsrA). Two plasmids encoding FliW and FliC or FliW and CsrA were transformed into *E. coli* BTH101 and used for FliW-FliC and FliW-CsrA interaction analysis. 1, 2, 4, and 8 µl of reporter strain were dotted on LB+IPTG+X-gal indication plates.

Fig. S2 Motility and growth profile of CD1015 and its derivative mutants.

(A) Growth profile in BHIS media. (B) Growth profile in TY media. (C) Swarming analysis on 0.2% BHIS agar plates. (D) Swimming analysis in 0.15% BHIS agar tubes.

Fig. S3 Disruption of FliC-FliW-CsrA enables improved utilization of mannose and trehalose.

(A-B) *C. difficile* growth in 10 and 20 mM mannose. (C-D) *C. difficile* growth in 5 and 10 mM trehalose.

Fig. S4 Δ*fliC*, Δ*fliW*, and Δ*csrA* mutants outcompete CD1015 in the presence of trehalose and mannose.

(A) Primers used for the colony PCR in the competition test. (B-D) Percentage of CD1015 in the total competition cultures. * means the significant difference of CD1015 CFU in the competition mixtures compared to that of at 0 h (*$P < 0.05$, **$P < 0.01$). One-way ANOVA with post-hoc Tukey test was used for statistical significance.

Fig. S5 Competition of CD1015 with Δ*fliC* analyzed by the colony PCR test.

Fifty colonies were selected and lysed for colony PCR test. Percentage of CD1015 accounting for the total bacteria was listed in the table. Experiments were repeated two times independently.

Fig. S6 Competition of CD1015 with Δ*fliW* analyzed by the colony PCR test.

Fifty colonies were selected and lysed for colony PCR test. Percentage of CD1015 accounting for the total bacteria was listed in the table. Experiments were repeated two times independently.

Fig. S7 Competition of CD1015 with Δ*csrA* analyzed by the colony PCR test.

Fifty colonies were selected and lysed for colony PCR test. Percentage of CD1015 accounting for the total bacteria was listed in the table. Experiments were repeated two times independently.

Fig. S8 Regulation of FliC-FliW-CsrA on *C. difficile* physiology.

Schematic representation of multiple roles of partner-switching mechanism FliC-FliW-CsrA in *C. difficile*.

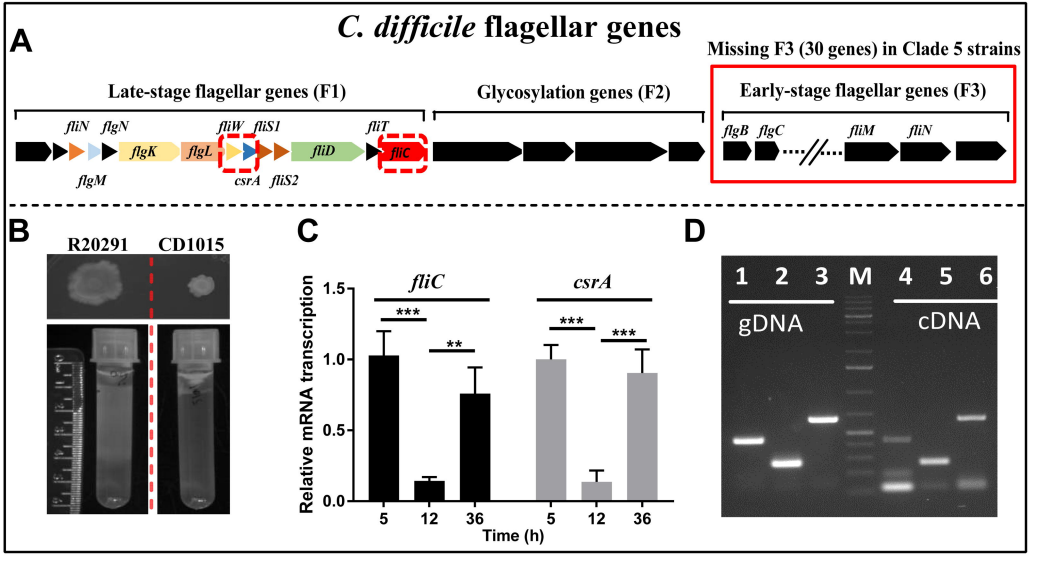
A
C. difficile flagellar genes
Missing F3 (30 genes) in Clade 5 strains
Late-stage flagellar genes (F1)
Glycosylation genes (F2)
Early-stage flagellar genes (F3)
fliN
flgN
flgK
flgL
fliW
fliS1
fliD
fliT
fliC
flgM
csrA
fliS2
flgB
flgC
fliM
fliN
B
R20291
CD1015
C
fliC
csrA
Relative mRNA transcription
1.5
1.0
0.5
0.0
***
**
***
***
5
12
36
5
12
36
Time (h)
D
1
2
3
M
4
5
6
gDNA
cDNA

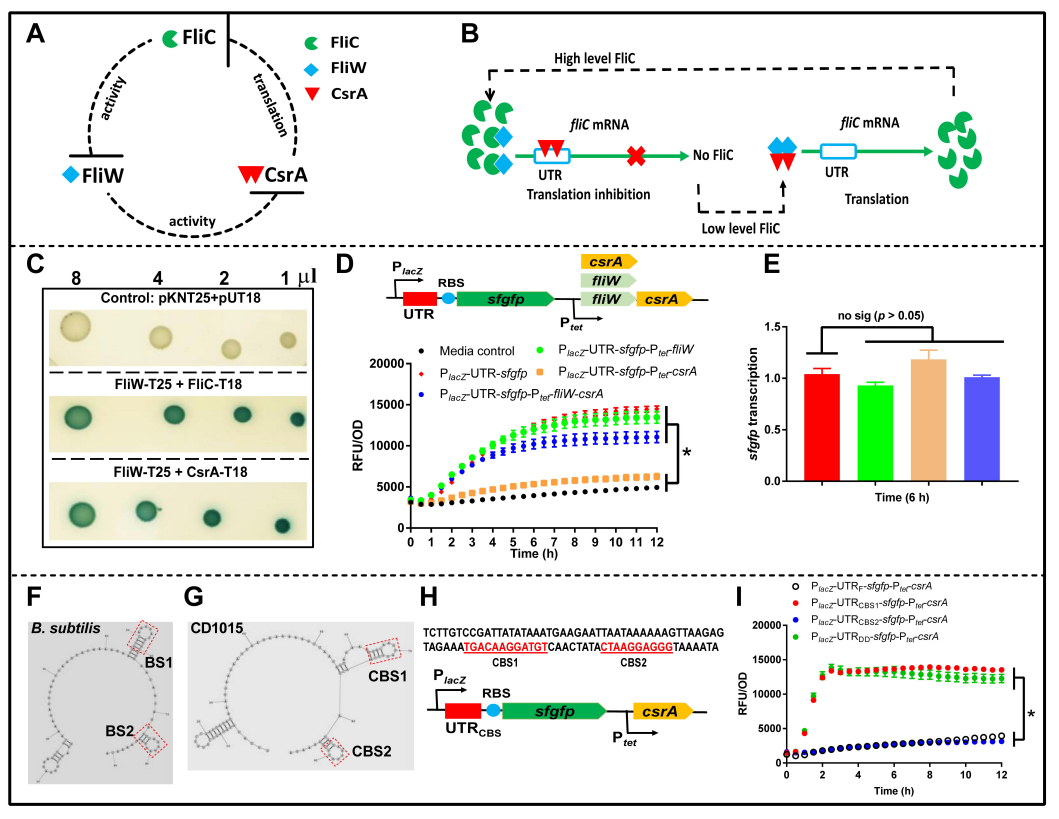
A
FliC
activity
translation
FliW
CsrA
activity
FliC
FliW
CsrA
B
High level FliC
fliC mRNA
UTR
Translation inhibition
No FliC
fliC mRNA
UTR
Translation
Low level FliC
C
8
4
2
1 μl
Control: pKNT25+pUT18
FliW-T25 + FliC-T18
FliW-T25 + CsrA-T18
D
PlacZ
RBS
UTR
sfgfp
csrA
fliW
fliW
csrA
Ptet
Media control
PlacZ-UTR-sfgfp
PlacZ-UTR-sfgfp-Ptet-fliW
PlacZ-UTR-sfgfp-Ptet-fliW-csrA
PlacZ-UTR-sfgfp-Ptet-csrA
RFU/OD
Time (h)
*
E
no sig (p > 0.05)
sfgfp transcription
Time (6 h)
F
B. subtilis
BS1
BS2
G
CD1015
CBS1
CBS2
H
TCTTGTCCGATTATATAAATGAAGAATTAATAAAAAAGTTAAGAG
TAGAAATGACAAGGATGTCAACTATACTAAGGAGGGTAAAATA
CBS1
CBS2
PlacZ
RBS
UTRCBS
sfgfp
csrA
Ptet
I
PlacZ-UTRF-sfgfp-Ptet-csrA
PlacZ-UTRCBS1-sfgfp-Ptet-csrA
PlacZ-UTRCBS2-sfgfp-Ptet-csrA
PlacZ-UTRDD-sfgfp-Ptet-csrA
RFU/OD
Time (h)
*

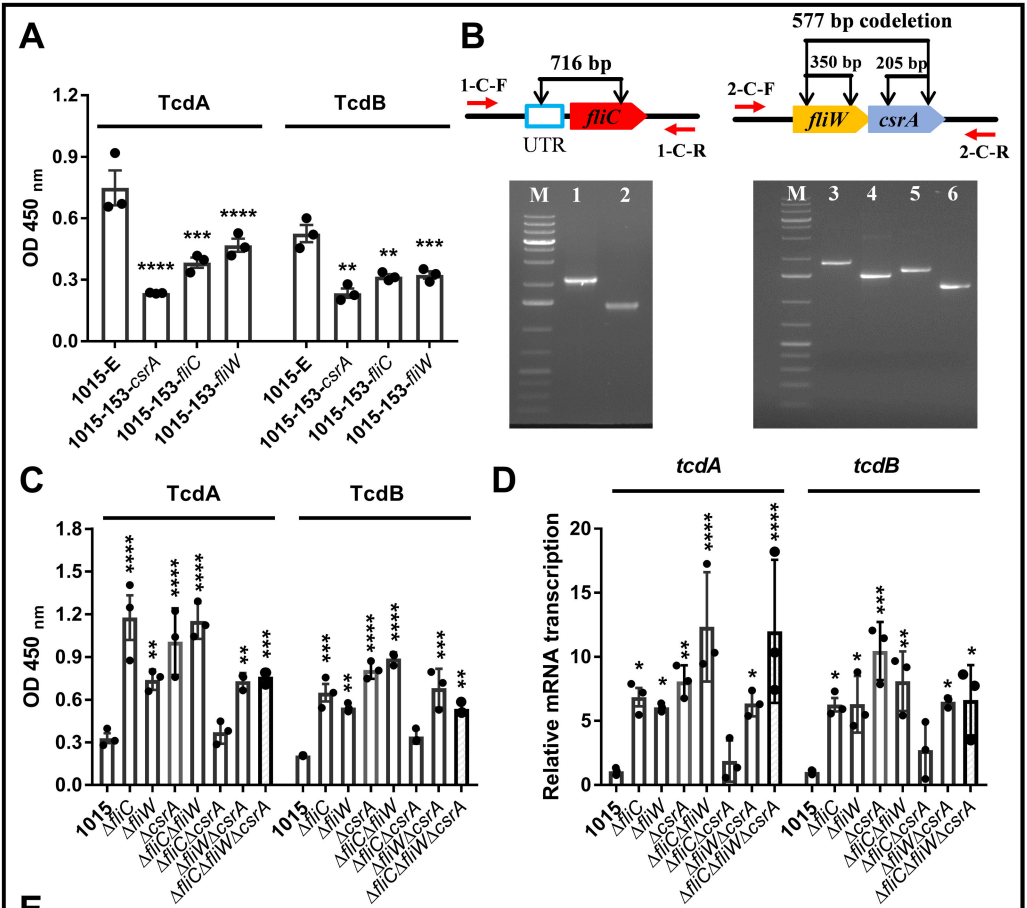

E

	Toxin (ELISA)		Gene expression	
Fold change	TcdA	TcdB	*tcdA*	*tcdB*
Δ*fliC*/1015	3.58*****	3.13***	6.85*	6.27*
Δ*fliW*/1015	2.25**	2.62**	6.05*	6.3*
Δ*csrA*/1015	3.06****	3.89****	8.08**	10.45***
Δ*fliC*Δ*fliW*/1015	3.5****	4.28****	12.34****	8.1**
Δ*fliC*Δ*csrA*/1015	1.13	1.64	1.87	2.72
Δ*fliW*Δ*csrA*/1015	2.22**	3.28***	6.36*	6.5*
Δ*fliC*Δ*fliW*Δ*csrA*/1015	2.31***	2.58**	11.99****	6.62*

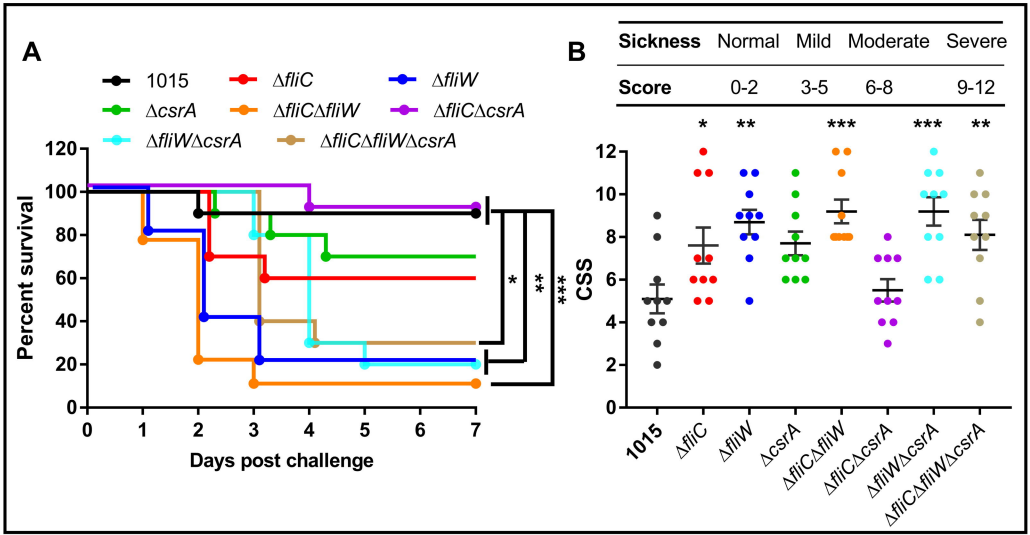
A
1015
ΔfliC
ΔfliW
ΔcsrA
ΔfliCΔfliW
ΔfliCΔcsrA
ΔfliWΔcsrA
ΔfliCΔfliWΔcsrA
Percent survival
Days post challenge
*
**
***
B
Sickness
Normal
Mild
Moderate
Severe
Score
0-2
3-5
6-8
9-12
CSS
1015
ΔfliC
ΔfliW
ΔcsrA
ΔfliCΔfliW
ΔfliCΔcsrA
ΔfliWΔcsrA
ΔfliCΔfliWΔcsrA

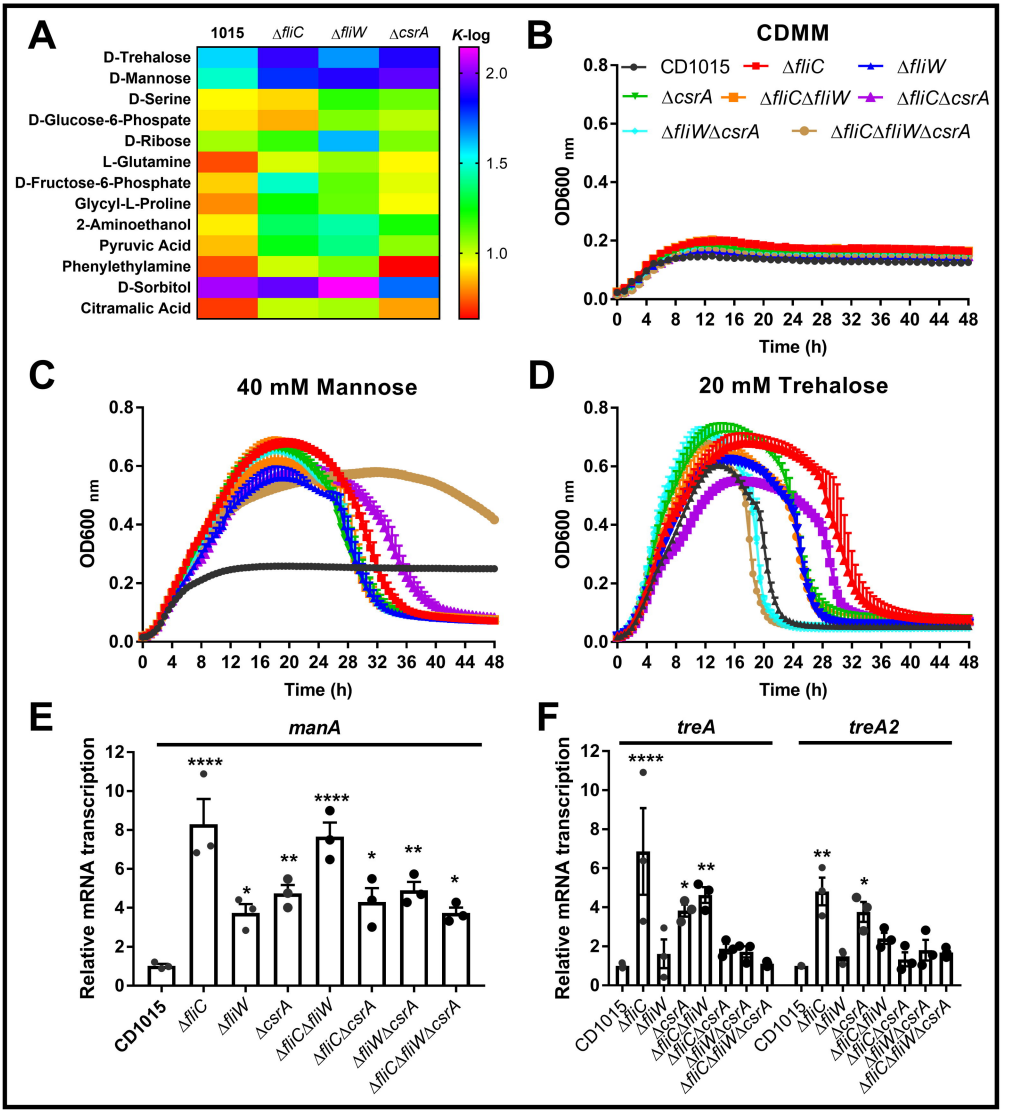
A
1015
ΔfliC
ΔfliW
ΔcsrA
K-log
D-Trehalose
D-Mannose
D-Serine
D-Glucose-6-Phospate
D-Ribose
L-Glutamine
D-Fructose-6-Phosphate
Glycyl-L-Proline
2-Aminoethanol
Pyruvic Acid
Phenylethylamine
D-Sorbitol
Citramalic Acid
2.0
1.5
1.0
B
CDMM
CD1015
ΔfliC
ΔfliW
ΔcsrA
ΔfliCΔfliW
ΔfliCΔcsrA
ΔfliWΔcsrA
ΔfliCΔfliWΔcsrA
OD600 nm
Time (h)
C
40 mM Mannose
OD600 nm
Time (h)
D
20 mM Trehalose
OD600 nm
Time (h)
E
manA
Relative mRNA transcription
CD1015
ΔfliC
ΔfliW
ΔcsrA
ΔfliCΔfliW
ΔfliCΔcsrA
ΔfliWΔcsrA
ΔfliCΔfliWΔcsrA
F
treA
treA2
Relative mRNA transcription
CD1015
ΔfliC
ΔfliW
ΔcsrA
ΔfliCΔfliW
ΔfliCΔcsrA
ΔfliWΔcsrA
ΔfliCΔfliWΔcsrA

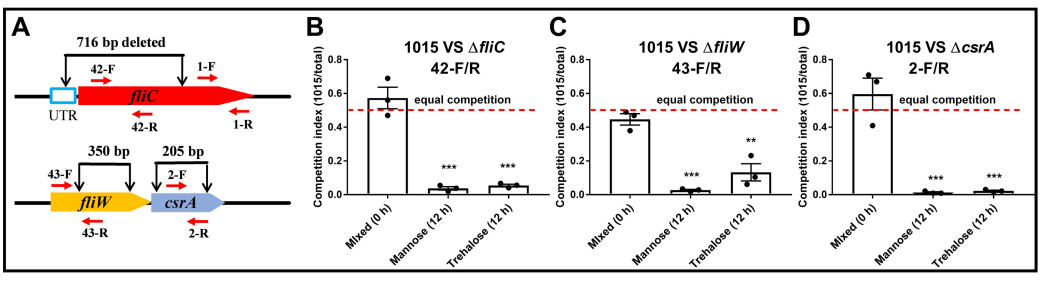
A
716 bp deleted
42-F
1-F
fliC
UTR
42-R
1-R
350 bp
205 bp
43-F
2-F
fliW
csrA
43-R
2-R
B
1015 VS ΔfliC
42-F/R
C
1015 VS ΔfliW
43-F/R
D
1015 VS ΔcsrA
2-F/R
Competition index (1015/total)
equal competition
***
**
Mixed (0 h)
Mannose (12 h)
Trehalose (12 h)

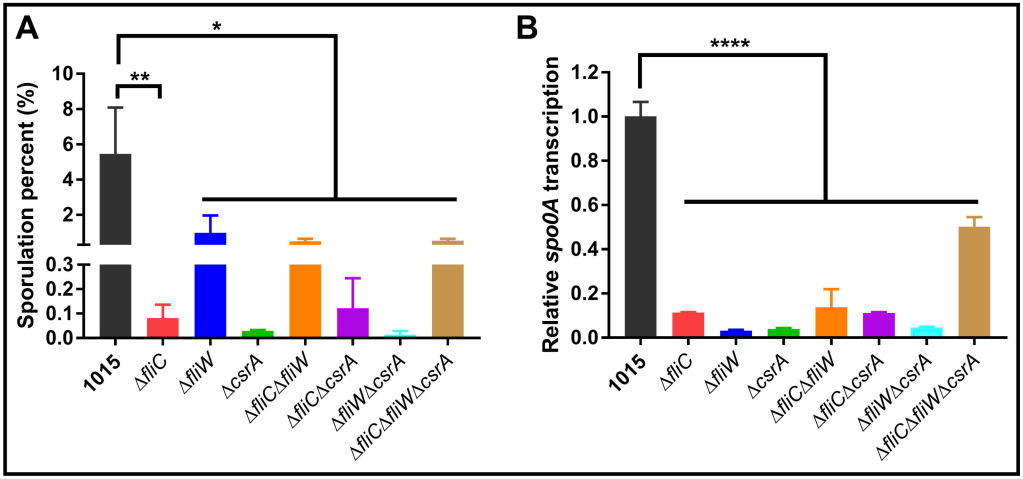
A
*
**
Sporulation percent (%)
10
8
6
4
2
0.3
0.2
0.1
0.0
1015
ΔfliC
ΔfliW
ΔcsrA
ΔfliCΔfliW
ΔfliCΔcsrA
ΔfliWΔcsrA
ΔfliCΔfliWΔcsrA
B
****
Relative spo0A transcription
1.2
1.0
0.8
0.6
0.4
0.2
0.0
1015
ΔfliC
ΔfliW
ΔcsrA
ΔfliCΔfliW
ΔfliCΔcsrA
ΔfliWΔcsrA
ΔfliCΔfliWΔcsrA